



Removal of patulin from aqueous solutions by propylthiol functionalized SBA-15

Michael Appell^{a,*}, Michael A. Jackson^b, Mary Ann Dombrink-Kurtzman^b

^a Bacterial Foodborne Pathogens and Mycology Research Unit, United States Department of Agriculture, Agricultural Research Service, National Center for Agricultural Utilization Research, 1815 N. University St., Peoria, IL 61604, USA¹

^b Renewable Product Technology Research Unit, United States Department of Agriculture, Agricultural Research Service, National Center for Agricultural Utilization Research, 1815 N. University St., Peoria, IL 61604, USA

ARTICLE INFO

Article history:

Received 21 October 2010

Received in revised form

14 December 2010

Accepted 2 January 2011

Available online 11 January 2011

Keywords:

Detoxification

SBA-15

Molecular Modeling

Mycotoxin

Patulin

ABSTRACT

Propylthiol functionalized SBA-15 silica was investigated to detoxify aqueous solutions contaminated with the regulated mycotoxin patulin. Micelle templated silicas with a specific pore size were synthetically modified to possess propylthiol groups, a functional group known to form Michael reaction products with the conjugated double bond system of patulin. BET surface area analysis indicated the propylthiol functionalized SBA-15 possesses channels with the pore size of 5.4 nm and a surface area of 345 m² g⁻¹. Elemental analysis indicates the silicon/sulfur ratio to be 10:1, inferring one propylthiol substituent for every ten silica residues. The propylthiol modified SBA-15 was effective at significantly reducing high levels of patulin from aqueous solutions (pH 7.0) in batch sorption assays at room temperature. The material was less effective at lower pH; however heating low pH solutions and apple juice to 60 °C in the presence of propylthiol functionalized SBA-15 significantly reduced the levels of patulin in contaminated samples. Composite molecular models developed by semi-empirical PM3 and empirical force field methods support patulin permeation through the mesoporous channels of propylthiol functionalized SBA-15. Density functional study at the B3LYP/6-31G(d,p) level predicts the proposed patulin adducts formed by reaction with the thiol residues exhibit less electrophilic properties than patulin. It is demonstrated the use of propylthiol functionalized SBA-15 is a viable approach to reduce patulin levels in aqueous solutions, including contaminated apple juice.

Published by Elsevier B.V.

1. Introduction

The adsorption and removal of toxicants from aqueous solutions can be complex, especially for natural toxins that can be produced at high levels by microorganisms. Patulin, **1**, is a regulated toxin biosynthesized by certain fungi which contaminate agricultural commodities, such as fruits, juices and other beverages (see Fig. 1) [1]. This toxin is primarily associated with the apple rotting fungus *Penicillium expansum*; however, several molds produce patulin including certain species of the *Aspergillus*, *Penicillium*, and *Byssoschlamys* genera [2]. Chronic exposure to high levels of this mycotoxin is associated with gastrointestinal diseases, teratogenicity, and carcinogenicity [2,3]. Maximum levels of patulin in apple juice and related products are recommended to be set at 50 μg kg⁻¹ by the Codex Committee on Food Additives and Contaminants and

many countries regulate and monitor apple-based juice products at this level [4]. A variety of methods exist to detect patulin varying in accuracy and rapidity, including HPLC analysis coupled with UV detection [4–6].

A broad range of post-harvest methods are employed to reduce patulin contamination of food and beverages [1,7]. Effective post-harvest methods include trimming and removal of contaminated parts of the fruit, resulting in contaminated waste [8]. In addition, several approaches have been studied to reduce patulin levels in aqueous solutions, such as juices and growth media. Certain strains of lactic acid bacteria were found to detoxify solutions contaminated with patulin and ochratoxin A [9]. Ascorbic acid reduces patulin levels under an oxygen environment; however this approach may be limited for packaged food products [10]. Patulin levels can be reduced by a variety of types of activated charcoal with potential impact on color and quality of the product [11]. Synthetic polyurethane-cyclodextrin nanosponge materials have been developed to sequester this toxin from aqueous media [12]. Select carbohydrates, specifically (1 → 3)-β-D-glucans and the (1 → 6)-β-D-glucans, are successful sorbents to bind a variety of mycotoxins, including patulin under basic conditions through non-covalent binding interactions [13]. There is need for more robust insoluble materials capable of detoxifying patulin contaminated

* Corresponding author. Tel.: +1 309 681 6249; fax: +1 309 681 6672.

E-mail address: michael.appell@ars.usda.gov (M. Appell).

¹ United States Department of Agriculture—Names are necessary to report factually on available data; however, the USDA neither guarantees nor warrants the standard of the product, and the use of the name by USDA implies no approval of the product to the exclusion of others that may also be suitable.

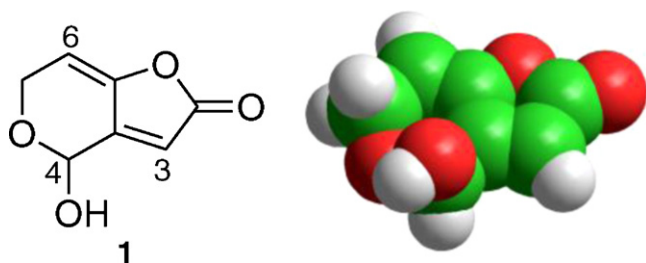


Fig. 1. Chemical structure and space filling model of patulin (1).

aqueous solutions. Herein, we report the development of a functionalized material capable of removing patulin from apple juice and other aqueous systems through covalent sequestration.

The toxic effects of patulin are due to the deleterious formation of adducts with important biomolecules, such as glutathione, cysteine residues of proteins, and DNA [3,14]. In fact, the electrophilic properties related to the conjugated double bond system of patulin have been utilized to reduce patulin levels by reaction with free thiols in solution. For example, thiol containing reducing agents increased the rate of patulin removal from contaminated alfalfa in rumen fluid [15]. In addition, cysteine has been investigated as an additive to detoxify patulin contaminated commodities [16]. However, these approaches leave patulin–thiol adducts free in solution with unknown properties or stabilities.

A promising field for the development of catalysts and other types of synthetic receptors is templated functionalized silicas tuned with specific pore sizes [17]. The mesoporous molecular sieve SBA-15 possesses a unique pore topology with hexagonally arranged adjacent mesoporous channels connected by micropore tunnels [18]. Specific applications of these types of nanoporous materials include catalyst supports, adsorbents, materials for size selective separations of small organics and proteins, and scaffolds for biosensors [17–20]. In this report, a SBA-15 silica is synthetically modified by reaction with 3-mercaptopropyltrimethoxysilane (MPTMS) to produce a thiol-modified material possessing mesoporous cavities suitable for patulin interaction. It is shown that the material is capable of removing high levels of patulin from aqueous solutions and the mechanism of action is probed by molecular modeling and quantum mechanical methods.

2. Experimental

2.1. Reagents and materials

Methanol, ethanol, acetone (HPLC grade), ethyl acetate (HPLC grade), hexane (HPLC grade), acetonitrile (HPLC grade), sodium phosphate, disodium phosphate, sodium acetate, glacial acetic acid, patulin, **1**, tetraethylorthosilicate (TEOS), 3-mercaptopropyltrimethoxysilane (MPTMS) and the templating molecule Pluronic P123 were obtained from Sigma–Aldrich, Inc. (Milwaukee, WI, USA).

2.2. Synthesis of SBA-15 functionalized silica

The sorbents were prepared by modifications of the methods described in the literature [21]. For SBA-15-PSH synthesis, 36 mmol tetraethylorthosilicate was dissolved in 125 ml of a 2 N HCl solution containing 3 wt.% Pluronic P123. This was stirred at 50 °C for 1 h. To the resulting suspension, 3.6 mmol 3-mercaptopropyltrimethoxysilane was added. This was stirred for an additional 90 min and was then aged at 90 °C for 16 h. The product was collected by filtration and washed with water, ethanol, and

methanol to remove excess template. The product was then dried *in vacuo* at 90 °C prior to analysis.

2.3. Materials characterization analytical methods

Sulfur analysis was performed on a Thermo Flash EA1112. Textural properties of the sorbents were calculated from nitrogen isotherms collected at 77 K using a Quantachrome Autosorb-1. Approximately 50 mg samples of the sorbents were degassed at 100 °C for 18 h for analysis. Surface areas were calculated using the multipoint BET method and pore sizes calculated using the BJH method on the adsorption branch. The solid phase CPMA¹³C NMR spectrum was recorded on a Bruker Avance 300 with a rotor speed of 3200 rpm.

2.4. LC-analysis

Patulin levels were determined by LC-analysis. The HPLC system consisted of a Shimadzu LC-20AT pump, a manual HPLC injector, a SPD-M20A diode array detector, a CBM-20A communications bus module, and a Phenomenex Luna 5 μ C18 100A column. Instrumentation was controlled by Shimadzu EZstart software. The LC-mobile phase consisted of 10% acetonitrile in water. Unless otherwise noted, patulin concentrations were calculated based on a standard curve using peak areas recorded at 276 nm. Patulin standard was stored in 1:1 acetonitrile/water (1 mg ml⁻¹). Patulin levels in spiked apple juice were evaluated following a previously published procedure [6] with the following modifications: Sep-Pak Vac 3cc (500 mg) C18 solid phase extraction columns were applied for sample clean-up, elution solvent was reduced by rotary evaporation, and injection was through a 20 μ l injection loop (0.05–5 μ g ml⁻¹, $r^2 = 0.975$).

2.5. Binding assays

SBA-15 and SBA-15-PSH were evaluated by measuring the capability to remove patulin from aqueous solutions in equilibrium binding assays. Assays were conducted in 1.5 ml silanized screw cap vials with a specified amount of SBA-15 or SBA-15-PSH in 1 ml solutions of patulin at various concentrations in 10 mM sodium phosphate buffer or 100% pure apple juice. Mesoporous silicas were evaluated at concentrations of 5 mg ml⁻¹ unless otherwise noted. For the room temperature experiments, vials were shaken on a Lab-line Multiwrist shaker set on speed 8 for the specified amount of time. Higher temperature assays were conducted in a Magni Whirl constant temperature bath with the shaker control set at 11. Experiments were performed in triplicate. Following incubation, the vials were centrifuged and the collected supernatant was filtered through Millex syringe driven PTFE filters (0.2 μ m). Removal efficiency from the equilibrium binding assays was determined by comparing the patulin peak area of samples run in the presence of the mesoporous silica with the patulin peak area of samples run without mesoporous silica through the following relationship:

$$\% \text{Removal efficiency} = \frac{(C_{\text{Standard}} - C_{\text{SBA-15}})}{C_{\text{Standard}}} \times 100 \quad (1)$$

where $C_{\text{SBA-15}}$ is concentration of the patulin recovered in the supernatant from the sample run with silica, and C_{Standard} is the concentration of the patulin standard without silica (0.05–50 μ g ml⁻¹, pH 7.0, $r^2 = 0.998$; pH 4.0, $r^2 = 0.997$) (0.05–5 μ g ml⁻¹, pH 9.0, $r^2 = 0.995$; pH 8.0, $r^2 = 0.999$; pH 6.0, $r^2 = 0.998$; pH 5.0, $r^2 = 0.997$; pH 3.0, $r^2 = 0.999$).

2.6. Molecular modeling

Molecular modeling was carried out using density functional theory, PM3 semi-empirical, and MM+ empirical methods. Density functional theory geometry optimization calculations were carried out using Parallel Quantum Solutions (Fayetteville, AR, U.S.A.) hardware and software v3.2 [22]. Molecular orbitals were modeled using the HyperChem v8.08 program (Gainesville, FL, U.S.A.) [23].

Composite models of the SBA-15 and SBA-15-PSH synthesized in this study were built based on previously published SBA-15 models [17,18] using the Hyperchem program v8.08 [23]. A layer of silica with the specified pore size was built using the PM3 semi-empirical method and MM+ force field, as implemented in Hyperchem. Components were initially optimized using the PM3 semi-empirical method. The model was built using the PM3 charges, the MM+ force field, and geometry optimization with the Polak–Ribiere conjugate gradient method. The depth of pore in the initial model was 9.1 Å, and the hexagonal pores were connected with layers of silica. Successive layers were added to develop a model with the depth of approximately 40 Å.

B3LYP density functional methods have provided insight into the structures patulin and related mycotoxins, and we applied this hybrid functional for the single molecule studies of patulin and proposed patulin–propylthiol adducts at the 6-31G(d,p) level [24–26]. Geometry optimization was performed in the gas phase using B3LYP/6-31G(d,p) level of theory on delocalized internal coordinates using the Eigenvector Following Algorithm with the convergence criteria set at 1×10^{-6} Hartree and a gradient of less than 3×10^{-4} a.u. Gauge Including Atomic Orbital (GIAO) methods were applied for shielding tensor calculations on geometry optimized structures of the propylthiol residue [27]. Results were evaluated as chemical shifts relative to the reference standard, tetramethylsilane. Frontier molecular orbitals were calculated and modeled using Hyperchem v8.08 with the default settings. The quantum chemical descriptors (orbital energy, gap energy, electronegativity, hardness, softness, and electrophilicity index) were calculated based on structures optimized at the B3LYP/6-31G(d,p) level as previously defined [28–30].

3. Results and discussion

3.1. Characterization of the propylthiol functionalized SBA-15

Elemental analysis studies indicate that the total sulfur content of the propylthiol functionalized SBA-15 (from here on SBA-15-PSH) to be 3.1%, which calculates to one propylthiol residue per 11 silica (SiO_2) residues (see Table 1). The nitrogen

Table 1

Composition and surface properties of the sorbents evaluated for removal of patulin from aqueous solutions.

| Sorbent | Surface area ($\text{m}^2 \text{g}^{-1}$) | Mean pore size (nm) | Pore volume (ml g^{-1}) | Wt.% S |
|------------|---------------------------------------------|---------------------|------------------------------------|--------|
| SBA-15 | 1336 | 9.0 | 1.83 | – |
| SBA-15-PSH | 345 | 5.4 | 0.45 | 3.10 |

Surface areas were obtained using the multipoint BET model. Pore size distributions were determined using the adsorption branch of the isotherm and the BJH method.

adsorption–desorption isotherms for the sorbents in this study are shown in Fig. 2. The transition in volume is sharp and the pore diameter peaks are relatively narrow indicating a moderately consistent population of pores with a narrow range of pore volumes and pore diameters. The median pore diameter is significantly reduced for the SBA-15-PSH (5.4 nm) compared to SBA-15 (9.0 nm). Modification of the SBA-15 with propylthiol substituents reduces the pore volume and surface area determined by BET analysis by approximately four-fold. The solid state carbon-13 chemical shifts of SBA-15-PSH matched the calculated values predicted by GIAO-B3LYP/6-31G(d,p) NMR analysis. Rotating the propylthiol chain had little effect on the calculated carbon chemical shifts compared to calculated chemical shifts for the straight chain propylthiol moiety. The properties of the SBA-15-PSH reported in this study compare favorably with related templated functionalized silicas [17]. Published TEM and HTREM micrographs of propylthiol functionalized SBA-15 with reagent ratios similar to the SBA-15-PSH reported here maintain the ordered morphology characteristic of mesoporous silicas synthesized in the presence of the Pluronic P123 template [17,31].

3.2. Modeling of SBA-15 and propylthiol functionalized SBA-15

Models of SBA-15 and SBA-15-PSH were built to gain insight into the influence of propylthiol substituents on the SBA-15 pores at the molecular level. A composite model was built based on physical parameters provided by the material characterization of the SBA-15 and SBA-15-PSH and previously published models of SBA-15 materials [17,18]. Specifically, we built the mesoporous channels using the experimentally determined pore diameters and previous published templated silica channel structures [18]. To simulate the imperfect nature of the silica channels, silicon–oxygen bonds were broken on the surface of the channels which provided hydrophilic silanol groups. For efficiency, atomistic scaffolds between the channels were built with 10 Å walls of silica and a length of 20 Å. The resulting model of SBA-15 is shown in Fig. 3(a), with a mesoporous honeycomb structure of ordered hexagonal channels. The unifor-

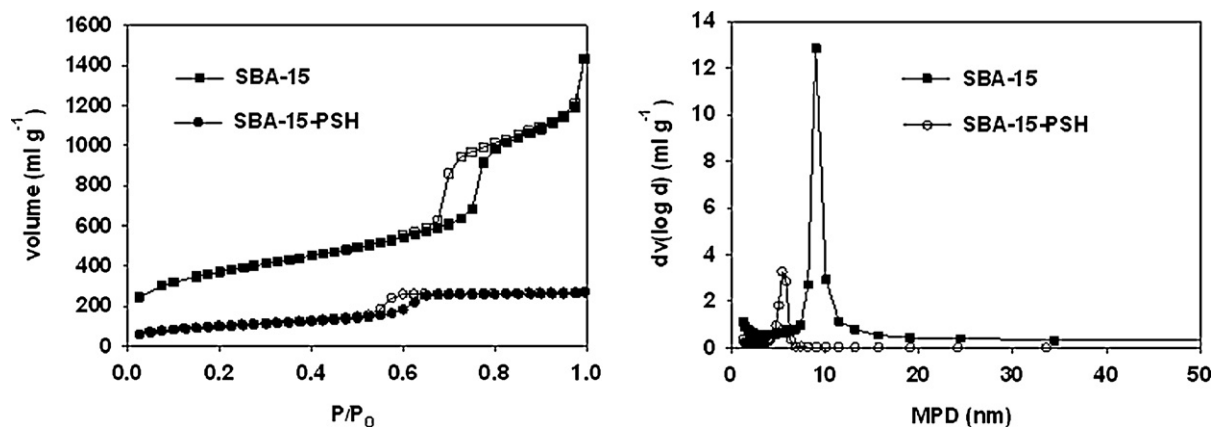


Fig. 2. Nitrogen adsorption–desorption isotherms at 77 K and resulting BJH mean pore diameters of SBA-15 and SBA-15-PSH. Solid symbols are the adsorption branches and open symbols are the desorption branches.

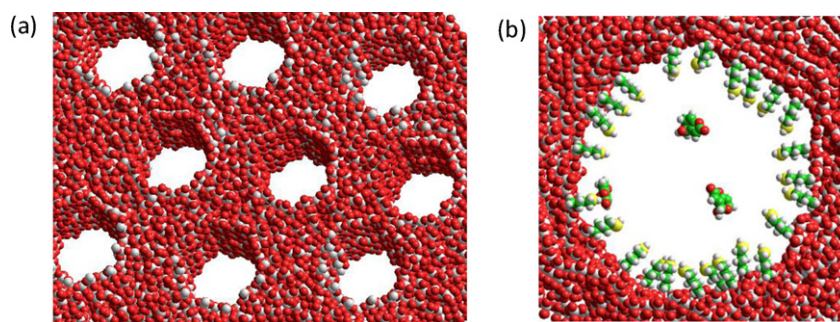


Fig. 3. (a) Cut-out view of a representative model of mesoporous SBA-15 with ordered hexagonal channels. Block size is $100 \text{ \AA} \times 70 \text{ \AA} \times 40 \text{ \AA}$. (b) Molecular 3D model of patulin molecules permeating a mesoporous silica channel of SBA-15-PSH.

mity and thickness of the silica walls between the channels are consistent with results reported by Bhattacharya et al., and this channel regularity agrees with the TEM results for SBA-15 [17]. The smaller pore diameter associated with the incorporation of propylthiol substituents in SBA-15 is apparent in the close-up model of propylthiol functionalized SBA-15 (see Fig. 3(b)). It should be noted that SBA-15 possesses deep channels and the models of SBA-15 and SBA-15-PSH are limited to 40 \AA blocks.

3.3. Removal of patulin by propylthiol functionalized SBA-15.

Initially, we investigated the ability of SBA-15 and SBA-15-PSH to act as a filter to remove patulin from contaminated aqueous solutions, such as apple juice or water. However, solid phase extraction columns filled with 25 mg of SBA-15 or SBA-15-PSH were unsuccessful at reducing patulin concentrations in buffered solutions (10 mM sodium phosphate, pH 7.0). The SBA-15-PSH was more effective as a solid sorbent additive to detoxify patulin contaminated solutions. Batch sorption results for assays carried out in 10 mM sodium phosphate solution are shown in Figs. 4–7. Fig. 4(a) provides the influence of time on a $5 \mu\text{g ml}^{-1}$ (5 ppm) solution of patulin in the presence of SBA-15 and SBA-15-PSH (5 mg) at pH 7.0. At 8 h, patulin is almost completely removed from solution in the presence of SBA-15-PSH. All other binding assay experiments reported here were carried out with 24-h incubation durations, which provided reproducible results over the range of concentrations studied.

The capacities of SBA-15 and SBA-15-PSH for high concentrations of patulin ($20 \mu\text{g ml}^{-1}$) at pH 7.0 are given in Fig. 4(b). Remarkably, 3 mg ml^{-1} of SBA-15-PSH is capable of removing 94% of patulin from high concentration samples. One generality observed in Fig. 4(a and b) is unmodified SBA-15 does not remove significant levels of patulin in the batch sorption assays. In contrast, the propylthiol functionalized SBA-15 exhibits a very large capacity for patulin, indicating the propylthiol residue is critical for removing patulin from solution in the batch sorption assay. Efforts to recover patulin from the used sorbent ($20 \mu\text{g ml}^{-1}$ patulin/5 mg SBA-15-PSH) with extraction (1 ml) by sonication for 15 min (acetonitrile $3\times$ and methanol $3\times$) recovered less than 0.1% of the calculated bound patulin. These results suggest the SBA-15-PSH covalently binds patulin and is capable of removing the toxin from solutions without leaching of bound patulin.

The binding properties of SBA-15-PSH over a range of patulin concentrations were determined by batch sorption experiments carried out in aqueous solutions (pH 7.0, 10 mM sodium phosphate buffer) at room temperature with 24-h incubation (see Fig. 5). SBA-15-PSH is capable of removing over 90% of patulin from aqueous solutions at pH 7.0 over concentrations $0.05\text{--}50 \mu\text{g ml}^{-1}$. Fig. 6 provides the relationship between pH and patulin removal by SBA-15-PSH. Patulin removal by SBA-15-PSH decreases at lower

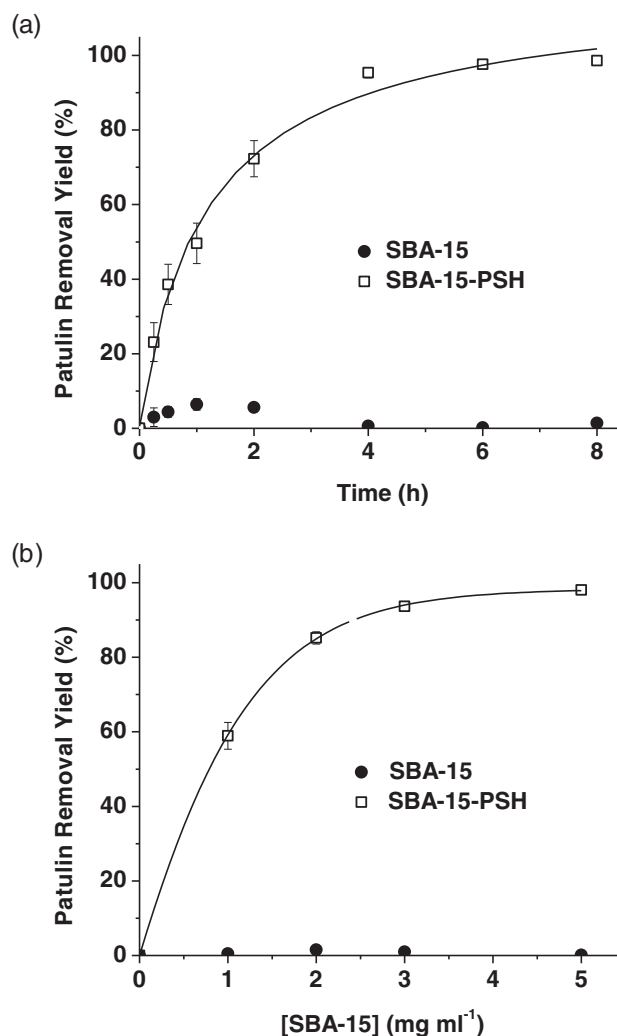


Fig. 4. (a) Time course patulin removal of SBA-15 and propylthiol functionalized SBA-15. $[\text{SBA-15}] = 5 \text{ mg ml}^{-1}$; $[\text{Patulin}]_{\text{Initial}} = 5 \mu\text{g ml}^{-1}$. Batch rebinding assays were conducted at room temperature for 24 h in sodium phosphate buffer (10 mM, pH 7.0). (b) Effect of concentrations of SBA-15 and SBA-15-PSH on patulin removal in buffer (10 mM sodium phosphate, pH 7.0). Experiments were conducted at room temperature and incubation for 24 h. $[\text{Patulin}]_{\text{Initial}} = 20 \mu\text{g ml}^{-1}$. The values are mean \pm standard deviation. Some values are smaller than the symbols.

pH values. However, we found heating the low pH solutions ($50 \mu\text{g ml}^{-1}$ patulin, pH 4.0) to 60°C increased patulin removal by 30% compared to experiments carried out at room temperature. The patulin binding properties of SBA-15-PSH at pH 4.0 were suitable for non-equilibrium Freundlich isotherm analysis for levels between 0.05 and $50 \mu\text{g ml}^{-1}$ and the sorption isotherm is pro-

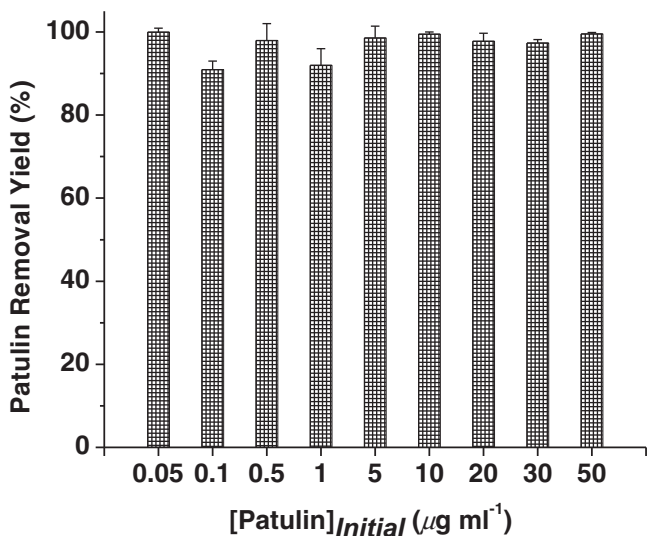


Fig. 5. Sorption of patulin by SBA-15-PSH in sodium phosphate buffer (10 mM, pH 7.0). Experiments were conducted at room temperature and 24-h incubation. The values are mean \pm standard deviation.

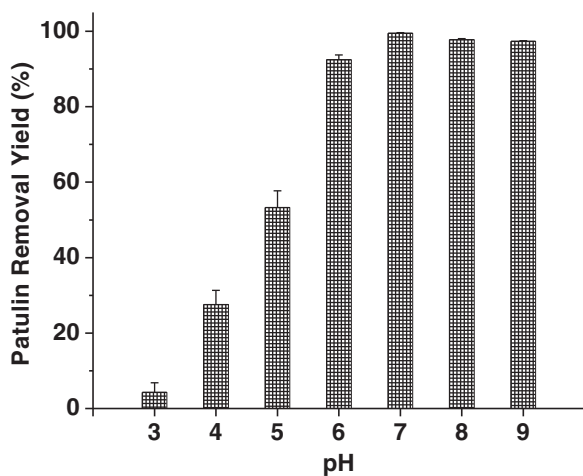


Fig. 6. Influence of pH on patulin removal by SBA-15-PSH in sodium phosphate buffer (10 mM). Experiments were conducted at room temperature and 24-h incubation. [SBA-15-PSH] = 5 mg ml⁻¹; [Patulin]_{Initial} = 5 µg ml⁻¹. The values are mean \pm standard deviation.

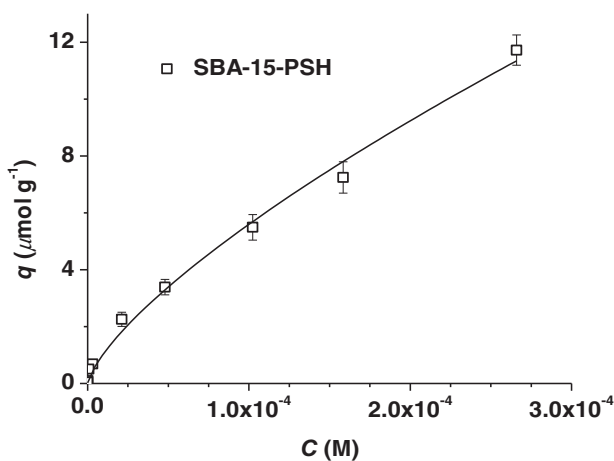


Fig. 7. Patulin sorption isotherm of SBA-15-PSH obtained in sodium phosphate buffer (10 mM, pH 4.0) at 60 °C. Incubation time was 24 h. C is concentration of free patulin, and q is the bound patulin per gram of SBA-15-PSH; $q = K_f C^{1/n}$, $K_f = 4330$ (µmol g⁻¹)(1 mol⁻¹)^{1/n}, $1/n = 0.72 \pm 0.04$; $r^2 = 0.995$. The values are mean \pm standard deviation.

Table 2
Reduction of patulin in apple juice by SBA-15-PSH.^a

| [Patulin] _{Initial} (µg ml ⁻¹) | % Patulin removed | [Patulin] _{Bound} ^b (µg) |
|-----------------------------------------------------|-------------------|----------------------------------------------|
| 5 | 34% | 1.71 \pm 0.07 |
| 1 | 37% | 0.37 \pm 0.06 |
| 0.5 | 42% | 0.21 \pm 0.01 |
| 0.1 | 72% | 0.072 \pm 0.009 |
| 0.05 | 48% | 0.024 \pm 0.002 |

^a Apple juice samples spiked with patulin were incubated for 24 h at 60 °C. Patulin levels were determined following an established procedure with solid phase extraction clean-up and HPLC–UV detection at 276 nm [6].

^b Mean \pm standard deviation.

vided in Fig. 7 [32,33]. Fitting to the Freundlich isotherm equation, $q = K_f C^{1/n}$, provides an average affinity and capacity (K_f) of 4330 (µmol g⁻¹)(1 mol⁻¹)^{1/n} and a Freundlich exponent of 0.72 ± 0.04 at 24 h incubation. The reduced activity of SBA-15-PSH at pH 4.0 may be attributed to the increased stability of patulin at lower pH and less favorable performance of the propylthiol functionalized SBA-15. It should be noted Michael addition reactions require a nucleophile, and the reactive species for SBA-15-PSH is the thiolate anion, which is less favored under acidic conditions.

Table 2 provides the effectiveness of SBA-15-PSH to remove patulin from contaminated apple juice. Experiments were carried out with 24-h incubation at 60 °C in the presence of 5 mg of SBA-15-PSH. Matrix effects and the acidic nature of apple juice may contribute to the decrease in effectiveness of SBA-15-PSH to remove patulin from apple juice compared to the buffered solution. The SBA-15-PSH is capable of lowering patulin levels in contaminated apple juice over a range of levels (0.05–5.0 µg ml⁻¹). The thiol functionalized material is effective at decontaminating apple juice at levels of concern (0.1 µg ml⁻¹) to below regulated levels (0.05 µg ml⁻¹). Overall, the SBA-15-PSH possesses high capacity for patulin and approaches the efficiency (24 h) and pH tolerance of biological methods to reduce mycotoxins, such as zearalenone detoxification by expression of the pZEA-1 plasmid in *Escherichia coli* [34].

3.4. Toxicological potential of patulin adducts

The toxicological potential of the adducts formed through the sequestration of patulin by the SBA-15-PSH was investigated using computational chemistry. Adducts formed by patulin and thiols have been extensively investigated, and a complex set of over 15 adducts have been isolated and characterized [35,36]. Based on published reports, two fundamental propylthiol–patulin adducts were studied using B3LYP/6-31(d,p) density functional methods to gain insight into the electrophilic properties important for reactivity of these species. It should be noted QSAR studies have predicted correlation between frontier orbital descriptors (LUMO) of soft electrophilic compounds and toxicity [37,38]. The LUMO and HOMO frontier orbitals of patulin and patulin adducts are provided in Fig. 8, and the molecular orbital and electrophilicity properties are given Table 3. Adduct 2 is based on the reaction of propylthiol with patulin at the C6 carbon. Proposed adduct 3 is a Michael addition-like intermediate at the C3 carbon of patulin. The HOMO and LUMO orbitals of patulin, 1, are primarily associated with the conjugated double bond system. In contrast the HOMO and LUMO frontier orbitals of adducts 2 and 3 include the thioether functional group with noticeable disruption of the conjugated system. The thiol adducts formed through disruption of the conjugated double bond system of patulin possess significantly dissimilar electronic properties compared to patulin. The proposed adducts possess a significantly lower global electrophilicity index, ω , compared to patulin, suggesting the proposed adducts are less reactive with biologically important soft nucleophiles. Similar patulin adducts

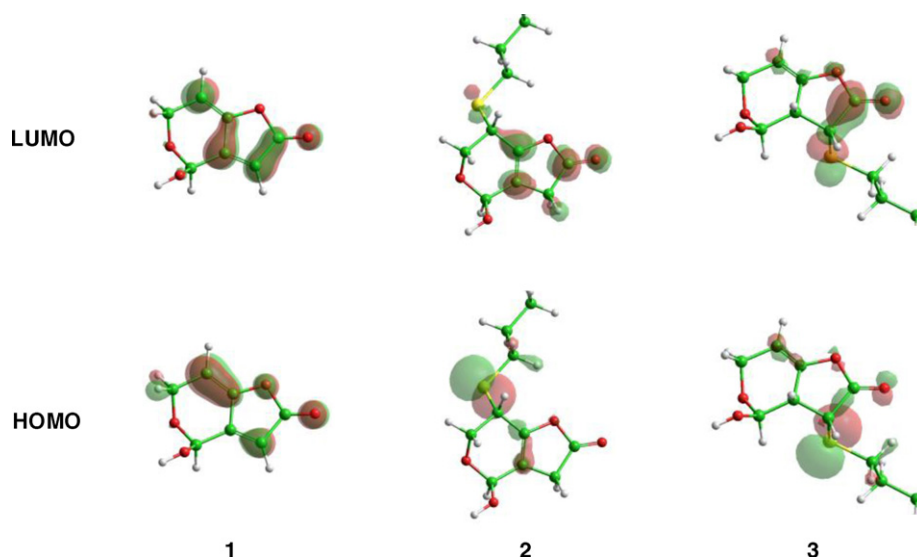


Fig. 8. Frontier molecular orbitals of patulin and patulin adducts calculated at the B3LYP/6-31G(d,p) level.

Table 3

HOMO, LUMO, gap energies, and electrophilicity parameters for patulin and patulin adducts geometry optimized at the B3LYP/6-31G(d,p) level.

| | 1 | 2 | 3 |
|---------------------|--------|--------|--------|
| LUMO+2 | 1.691 | 0.920 | 0.838 |
| LUMO+1 | 1.385 | 0.334 | 0.473 |
| LUMO | -2.051 | -0.599 | -0.571 |
| HOMO | -6.588 | -6.024 | -6.230 |
| HOMO-1 | -7.454 | -6.595 | -6.601 |
| HOMO-2 | -7.941 | -7.486 | -7.400 |
| $\Delta\varepsilon$ | 4.537 | 5.425 | 5.659 |
| χ | -4.320 | -3.312 | -3.401 |
| η | 2.269 | 2.713 | 2.830 |
| σ | 0.441 | 0.369 | 0.353 |
| ω | 4.112 | 2.021 | 2.043 |

All HOMO and LUMO energies reported in electron volt (eV). Band gap energy, $\Delta\varepsilon$, is given eV, and is defined $\Delta\varepsilon = (\varepsilon_{\text{LUMO}} - \varepsilon_{\text{HOMO}})$. Electronegativity, χ , is in eV and calculated by the following relationship $\chi = -(\varepsilon_{\text{LUMO}} + \varepsilon_{\text{HOMO}})/2$. Hardness, η , is in eV and is half of the band gap energy. Softness, σ , is in eV^{-1} , and calculated by $\sigma = 2/(\varepsilon_{\text{LUMO}} - \varepsilon_{\text{HOMO}})$. Electrophilicity index, ω , is calculated by $\omega = \chi^2/2\eta$.

formed from free cysteine residues have been shown to be less toxic than patulin [15,16]. An advantage SBA-15-PSH has over the use of free thiols to detoxify patulin contaminated solutions is the SBA-15-PSH removes patulin from solution or juice and sequesters the patulin adducts within the mesoporous silica.

4. Summary and conclusion

A propylthiol modified SBA-15 is developed as an approach to detoxify aqueous commodities contaminated with patulin. The effectiveness of the SBA-15-PSH to reduce patulin levels is sensitive to pH and time, and large quantities of material (5 mg ml^{-1}) are able to detoxify large concentrations of patulin. In addition, the material was suitable to reduce patulin from acidic solutions and apple juice with 24-h incubation at 60°C . A composite model was built based on the characterization of the SBA-15-PSH material, and SBA-15 modeling studies carried out by other groups. Molecular modeling provided insight into the effects of synthetic modification on the pore size of mesoporous SBA-15. The SBA-15-PSH is useful to reduce levels of patulin in contaminated apple juice and other aqueous solutions.

Acknowledgments

The authors thank Judy Blackburn and Lijuan C. Wang for excellent technical assistance. Dr. Charles Mullen of the USDA-ARS-Eastern Regional Research Center performed the sulfur analyses. Robert Caughey of the University of Illinois College of Medicine at Peoria assisted with the materials characterization. The authors thank the anonymous reviewers for their comments. Mention of trade names or commercial products in this article is solely for the purpose of providing specific information and does not imply recommendation or endorsement by the U.S. Department of Agriculture. USDA is an equal opportunity provider and employer.

References

- [1] M.M. Moake, O.I. Padilla-Zakour, R.W. Worobo, Comprehensive review of patulin control methods in foods, *Comp. Rev. Food Sci. Food Saf.* 4 (2005) 8–21.
- [2] L. Jackson, M.A. Dombrink-Kurtzman, Patulin, in: G.M. Sapers, J.R. Gorney, A.E. Yousef (Eds.), *Microbiology of Fruits and Vegetables*, CRC Press, Boca Raton, 2006, pp. 281–311.
- [3] D.M. Schumacher, C. Müller, M. Metzler, L. Lehmann, DNA–DNA cross-links contribute to the mutagenic potential of the mycotoxin patulin, *Toxicol. Lett.* 166 (2006) 268–275.
- [4] I.K. Cigić, H. Prosen, An overview of conventional and emerging analytical methods for the determination of mycotoxins, *Int. J. Mol. Sci.* 10 (2009) 62–115.
- [5] D.R. Katerere, S. Stockenström, G. Balducci, G.S. Shephard, Determination of patulin in apple juice: comparative evaluation of four analytical methods, *J. AOAC Int.* 90 (2007) 162–166.
- [6] J.-K. Li, R.-N. Wu, Q.-H. Hu, J.-H. Wang, Solid-phase extraction and HPLC determination of patulin in apple juice concentrate, *Food Control* 18 (2007) 530–534.
- [7] M.W. Trucksess, P.M. Scott, Mycotoxins in botanicals and dried fruits: a review, *Food Addict. Contam.* 25 (2008) 181–192.
- [8] S. Bandoh, K. Higashihara, M. Takeuchi, K. Ohsawa, T. Goto, Physical protection of apple products from patulin contamination, in: M. Appell, D.F. Kendra, M.W. Trucksess (Eds.), *American Chemical Society Symposium Series 1031, Mycotoxin Prevention and Control in Agriculture*, American Chemical Society, Washington, DC, 2009, pp. 69–76.
- [9] S. Fuchs, G. Sontag, R. Stidl, V. Ehrlich, M. Kundi, S. Knasmüller, Detoxification of patulin and ochratoxin A, two abundant mycotoxins, by lactic acid bacteria, *Food Chem. Toxicol.* 46 (2008) 1398–1407.
- [10] S. Drusch, S. Kopka, J. Kaeding, Stability of patulin in a juice-like aqueous model system in the presence of ascorbic acid, *Food Chem.* 100 (2007) 192–197.
- [11] N.L. Leggett, G.S. Shephard, S. Stockenström, E. Staal, D.J. van Schalkwyk, The reduction of patulin in apple juice by three different types of activated carbon, *Food Addict. Contam.* 18 (2001) 825–829.
- [12] M. Appell, M.A. Jackson, Synthesis and evaluation of cyclodextrin-based polymers for patulin extraction from aqueous solutions, *J. Mol. Incl. Phenom. Macrocycl. Chem.* 68 (2010) 117–122.
- [13] A. Yiannikouris, G. André, L. Poughon, J. François, C.-G. Dussap, G. Jeminet, G. Bertin, J.-P. Jouany, Chemical and conformational study of the interactions involved in mycotoxin complexation with β -D-glucans, *Biomacromolecules* 7 (2006) 1147–1155.

- [14] R. Fliege, M. Metzler, Electrophilic properties of patulin. N-acetylcysteine and glutathione adducts, *Chem. Res. Toxicol.* 13 (2000) 373–381.
- [15] D.P. Morgavi, H. Boudra, J.-P. Jouany, D. Graviou, Prevention of patulin toxicity on rumen microbial fermentation by SH-containing reducing agents, *J. Agric. Food Chem.* 51 (2003) 6906–6910.
- [16] S. Lindroth, A. von Wright, Detoxification of patulin by adduct formation with cysteine, *J. Environ. Pathol. Toxicol. Oncol.* 10 (1990) 254–259.
- [17] S. Bhattacharya, B. Coasne, F.R. Hung, K.E. Gubbins, Modeling micelle-templated mesoporous material SBA-15: atomistic model and gas adsorption studies, *Langmuir* 25 (2009) 5802–5813.
- [18] A.L. Doadrio, J.C. Doadrio, J.M. Sánchez-Montero, A.J. Salinas, M. Vallet-Regi, A rational explanation of the vancomycin release from SBA-15 and its derivative by molecular modelling, *Micropor. Mesopor. Mater.* 132 (2010) 559–566.
- [19] T.X. Bui, H. Choi, Adsorptive removal of selected pharmaceuticals by mesoporous silica SBA-15, *J. Hazard. Mater.* 168 (2009) 602–608.
- [20] J. Aguado, J.M. Arsuaga, A. Arencibia, M. Lindo, V. Gascón, Aqueous heavy metals removal by adsorption on amine-functionalized mesoporous silica, *J. Hazard. Mater.* 163 (2009) 213–221.
- [21] J.M. Arsuaga, A. Arencibia, Influence of synthesis conditions on mercury adsorption capacity of propylthiol functionalized SBA-15 obtained by co-condensation, *Micropor. Mesopor. Mater.* 109 (2008) 513–524.
- [22] Parallel Quantum Solutions, <http://www.pqs-chem.com>.
- [23] Hypercube, Inc. <http://www.hyper.com>.
- [24] L. Türker, S. Gümüş, A theoretical study on vomitoxin and its tautomers, *J. Hazard. Mater.* 163 (2009) 285–294.
- [25] M. Appell, M.A. Dombrink-Kurtzman, D.F. Kendra, Comparative study of patulin, ascladiol, and neopatulin by density functional theory, *Theochem* 894 (2009) 23–31.
- [26] L. Türker, S. Gümüş, Quantum chemical treatment of nivalenol and its tautomers, *J. Hazard. Mater.* 153 (2008) 329–339.
- [27] K. Wolinski, J.F. Hinton, P. Pulay, Efficient implementation of the gauge-independent atomic orbital method for NMR chemical shift calculations, *J. Am. Chem. Soc.* 112 (1990) 8251–8260.
- [28] P.K. Chattaraj, U. Sarkar, D.R. Roy, Electrophilicity index, *Chem. Rev.* 106 (2006) 2065–2091.
- [29] R.M. LoPachin, T. Gavin, B.C. Geohagen, S. Das, Neurotoxin mechanisms of electrophilic type-2 alkenes: soft–soft interactions described by quantum mechanical parameters, *Toxicol. Sci.* 98 (2007) 561–570.
- [30] G. Madjarova, A. Tadjer, Tz.P. Cholakova, A.A. Dobrev, T. Mineva, Selectivity descriptors for the Michael addition reaction as obtained from density functional based approaches, *J. Phys. Chem. A* 109 (2005) 387–393.
- [31] R.P. Hodgkins, A.E. Garcia-Bennett, P.A. Wright, Structure and morphology of propylthiol-functionalised mesoporous silicas templated by non-ionic triblock copolymers, *Micropor. Mesopor. Mater.* 79 (2005) 241–252.
- [32] M.R. Pérez-Gregorio, M.S. García-Falcón, E. Martínez-Carballo, J. Simal-Gándara, Removal of polycyclic aromatic hydrocarbons from organic solvents by ashes wastes, *J. Hazard. Mater.* 178 (2010) 273–281.
- [33] Y. Yoon, P. Westerhoff, S.A. Snyder, M. Esparza, HPLC-fluorescence detection and adsorption of bisphenol A, 17 β -estradiol, and 17 α -ethynyl estradiol on powdered activated carbon, *Water Res.* 37 (2003) 3530–3537.
- [34] A.D. Altalhi, B. El-Deeb, Localization of zearalenone detoxification gene(s) in pZEA-1 plasmid of *Pseudomonas putida* ZEA-1 and expressed in *Escherichia coli*, *J. Hazard. Mater.* 161 (2009) 1166–1172.
- [35] N.H. Schebb, H. Faber, R. Maul, F. Heus, J. Kool, H. Irth, U. Karst, Analysis of glutathione adducts of patulin by means of liquid chromatography (HPLC) with biochemical detection (BCD) and electrospray ionization tandem mass spectrometry (ESI-MS/MS), *Anal. Bioanal. Chem.* 394 (2009) 1361–1373.
- [36] R. Fliege, M. Metzler, Electrophilic properties of patulin: adduct structures and reaction pathways with 4-bromothiophenol and other model nucleophiles, *Chem. Res. Toxicol.* 13 (2000) 363–372.
- [37] B. Cai, L. Xie, D. Yang, J.-P. Arcangeli, Toxicity evaluation and prediction of toxic chemicals on activated sludge system, *J. Hazard. Mater.* 177 (2010) 414–419.
- [38] S. Kar, K. Roy, QSAR modeling of toxicity of diverse organic chemicals to *Daphnia magna* using 2D and 3D descriptors, *J. Hazard. Mater.* 177 (2010) 344–351.